

Landslides

DOI 10.1007/s10346-018-1037-6

Received: 6 January 2018

Accepted: 3 July 2018

© Springer-Verlag GmbH Germany
part of Springer Nature 2018

Qigen Lin · Ying Wang

Spatial and temporal analysis of a fatal landslide inventory in China from 1950 to 2016

Abstract Landslides result in severe casualties every year in China. However, there are few historical fatal landslide catalogs available to quantitatively assess the impact as well as the temporal and spatial patterns of landslides. The Fatal Landslide Event Inventory of China (FLEIC), which spans from 1950 to 2016, was compiled based on multiple data sources. The inventory contains 1911 non-seismically triggered landslides, which resulted in a total of 28,139 deaths in China during 1950–2016. The occurrence frequency of fatal landslides presented significantly different trends for different grades of events. Very large fatal landslide events (fatalities ≥ 30) were on the rise during 1950–1999 and declined from 2000 to 2016. The decreasing trend after 2000 can be attributed to the increase in landslide mitigation investments. The small and medium-sized fatal landslide events (fatalities < 10) showed a significant increasing trend between 1950 and 2016, especially during the period of 2000–2016. This significant increasing trend is partly due to the improvement of the availability of landslide data online and may also be related to other factors including an increase in extreme precipitation events, the effects of land urbanization, and so on. This suggested that the inherent incompleteness of the landslide time series should be considered when analyzing. The fatal landslides mainly occurred between April and September (82.15%), which is consistent with the monthly precipitation variation in China. Spatially, most of the fatal landslides occurred in 14 provinces: five southwestern provinces (Yunnan, Sichuan, Guangxi, Guizhou, and Chongqing), five southeastern provinces (Hunan, Guangdong, Fujian, Jiangxi, and Zhejiang), Shaanxi and Shanxi, Hubei and Gansu. These 14 provinces account for 86% of the total fatal landslides and their associated fatalities. **The spatial association between the fatal landslide density and possible influencing factors was assessed based on a geographical detector method. The results showed that the interacting factors between the precipitation and topography, soil, lithology, vegetation and population density are more closely related to the spatial distribution of fatal landslides than each individual factor.**

Keywords Fatal landslide · Inventory · Spatiotemporal patterns · China · **Geographical detector method**

Introduction

China is one of the countries that experiences a severe loss of life as a result of landslides (Petley 2012; Lin et al. 2017a, b). The statistics of the China Statistical Yearbook show that 373,630 landslides occurred in China, which resulted in 10,996 total deaths, with approximately 690 fatalities per year during 2000–2015 (Sheng et al. 2016). Moreover, the occurrence of landslide disasters is on the rise for three main reasons (Gariano and Guzzetti 2016). First, the excessive exploitation of natural resources and vegetation damage has increased the instability of the surface soil (Nadim et al. 2006). Second, land urbanization, especially

mountainous urbanization, increases the exposed population (Li et al. 2017). Third, an increase in extreme precipitation in China has been found, and the areas experiencing unusually extreme precipitation are also increasing (Fu et al. 2013). For cases that recently occurred, a landslide occurred on June 24, 2017 in Diexi, Mao County, Sichuan Province of southwestern China due to continuous rainfall. This landslide caused approximately 120 deaths (MLRC 2017). Another rainfall triggered landslide killed 23 people on July 1, 2016 in Pianpo Village, Dafang County, Guizhou Province of China (CIGEM 2016).

However, the losses resulting from landslide disasters are often underestimated, which leads to an unrealistic understanding of landslide disaster risk. The main reasons for the underestimation of damages caused by landslides are difficulties observing the occurrence of landslides, which result from the local impact of landslides and lack of disaster monitoring networks, such as those for earthquakes and typhoons. In addition, losses caused by disasters are usually registered as the cause resulting in the damage caused by the landslide is often registered to an earthquake, typhoon, or flood (Kirschbaum et al. 2015). Therefore, it is key to accurately understand landslide disaster risk by developing and analyzing the historical landslide inventory.

Landslide inventories are critical step to understand, track and analyze landslide disasters, and provide a foundation for landslide hazard, vulnerability, and risk assessment. They can be divided into event-based and historical inventories (Klose et al. 2015). Event-based database refers to landslides caused by a triggering factor (earthquake, typhoon, etc.). Such databases are often used to analyze the causes and effects of a single disaster event. Historical landslide catalogs constitute a pool of data on landslides and can be divided into global, continental, national, and regional scales according to the landslides that occurred in certain areas (Guzzetti et al. 2012; Klose et al. 2015). On a global scale, Kirschbaum et al. (2015) established a global landslide catalog covering the period of 2007 to 2013. Based on where and when the landslides happened, the temporal and spatial distribution was analyzed. The results showed that landslides were reported most frequently from July to September. Most events occurred in Asia, North America, and Southeast Asia. Petley (2012) compiled a global fatal landslide database for the period from 2004 to 2010. The method of running mean and spatial analysis were adopted to investigate the spatiotemporal patterns. The results showed that hotspots of global fatal landslides (causing death) are concentrated in China, south Asia, southeast Asia, Latin America, and the Caribbean. Such spatial concentration dominates the annual landslide cycle, which is highest in the summer in the northern hemisphere (Petley 2012; Kirschbaum et al. 2015). On a continental scale, Sepúlveda and Petley (2015) built a fatal landslide database of Latin America and the Caribbean during 2004–2013, and analyzed its spatial distribution. The fatal landslides mainly occurred in Haiti, Central America, Colombia, and southeastern Brazil.

Moreover, by comparing the frequency of landslides in El Niño and La Niña event years with that in common years, the effect of El Niño-Southern Oscillation (ENSO) on landslide occurrence was discussed. Their finding showed that ENSO has a significant effect on the interdecadal fluctuations in the occurrence frequency of fatal landslides in this area. Haque et al. (2016) collected 476 deadly landslides for 27 European countries during 1995–2014 and analyzed the spatiotemporal distribution using space-time pattern mining tools in ArcGIS Pro 1.1; the results of this study showed that fatal landslides are on the rise in Europe, with landslides causing the most deaths in Turkey, Italy, Russia, and Portugal. On a national scale, Guzzetti (2000) compiled a landslide database of Italy for the period from 1279 to 1999 and assessed the risk of landslides in Italy. The results showed that the areas where the landslides frequently occurred were mainly located in the northern Alpine region and the southern Campania area. The frequency of landslides against their resulting fatalities plots for Italy were used to compare those for Alps, Canada, Japan, China, and Hong Kong. The result showed that the frequency in Italy was higher than in the Alps, Canada, and Hong Kong, but lower than that of Japan and China. The national landslide database of Great Britain has been developed by Pennington et al. (2015) and enriched by Taylor et al. (2015). Then, this landslide database was applied to national daily landslide hazard assessment and landslide domain mapping. Damm and Klose (2015) established a landslide database of Germany and discussed the database application for analyzing landslide frequency and causes, impact statistics, and modeling landslide susceptibility. Klose et al. (2016) further assessed the landslide impacts on infrastructure and society using three case studies from Germany landslide database. Pereira et al. (2016) compiled a catalog of 281 fatal landslides in Portugal between 1865 and 2010. Based on this database, the authors analyzed the spatiotemporal distribution of landslide frequency and fatalities, and assessed the mortality risk by mean annual average mortality rate. They found that landslide fatalities mainly occurred in the north of the Tagus valley. Besides, the landslide mortality rate shows a slight upward trend in the Portuguese regions. There are 22 out of 37 countries that have national landslide databases in Europe (Van Eeckhaut and Hervás 2012).

However, there is still no complete historical fatal landslide database for China. Li et al. (2016) collected 1221 historical landslides from 1949 to 2011 and analyzed the spatial distribution of landslides. However, the losses (deaths, injured, and missing persons) caused by the landslides were not considered, which is important for landslide risk assessment and management. Although the Durham Fatal Landslide Database is used for the analysis of fatal landslides in Asia (Petley 2010), the global landslide database developed by Petley (2012) and Kirschbaum et al. (2015) that contains some fatal landslide events in China, these databases are incomplete of data for non-English-speaking countries such as China, because the collection of such databases were based on English media. In addition, the shorter time coverage (less than 10 years) of such databases may limit temporal trend analyses.

In this paper, we attempt to bridge this gap by developing a complete Fatal Landslide Event Inventory of China (FLEIC) for the period from 1950 to 2016. Then, the temporal trends and spatial

distribution of fatal landslides of China in the past 60 years were quantitatively assessed, and the cause was discussed. Finally, the spatial association between fatal landslide density and possible influencing factors was explored.

Material and methods

Fatal landslide event inventory of China

The landslide events that caused loss of life (fatal landslide events) in China for the period from 1950 to 2016 were collected from multiple sources including a geological hazard event dataset in China (1949–2008), geological stress and geological disaster data in China and neighbor region (1950–1998), the China Geological Hazard Bulletin, Reports on the Geological Disaster Situation, the Yesterday Disaster Report, media reports, and the literature. The term “landslide” in this paper refers to the wider definition of the landslide including landslides, rock falls, and debris flows, which are the three major land mass wasting movements that result in fatalities in China. A fatal landslide event in this paper refers to a single landslide causing one death or multiple deaths. The main process for compiling the FLEIC is as follows.

The fatal landslide events collected from different sources were documented, and the duplicated events were removed through proofreading. Each fatal landslide event is characterized by ten fields, including ID, date, location, latitude, longitude, radius of confidence, landslide type, fatality, trigger, and sources, which are shown in Table 1. The method developed by Kirschbaum et al. (2010) for landslide event compilation was applied to determine the latitude, longitude, and radius of confidence. The latitudes and longitudes were obtained based on Google Earth (<http://www.earth.google.com>) and other online maps (<http://www.gpspg.com/maps.htm>). The radius of confidence, i.e., spatial precision, was calculated based on the geographic location description of each fatal landslide event. For example, the most accurate geographical location of fatal landslide 85 is Tonglu County. Tonglu County covers an area of 1825 km². Assuming that the spatial range of Tonglu County is roughly circular, a radius of 24.12 km can be obtained based on the circle area calculation formula. This means that fatal landslide 85 may be located in a circle with a radius of 24.12 km, and the radius of confidence of event 85 in Table 1 is less than 25 km. The field date is the day when the fatal landslide occurred. If the description of the date is a fatal landslide triggered by continuous rainfall during the multi-day process, the intermediate date of the rainfall process is recorded as the date of the landslide occurrence. Classification of landslide type was difficult due to some of the data sources, such as media reports lacking a detailed landslide description. Therefore, we classified the landslides into three types: generic shallow landslide, rock fall, and debris flow. The trigger of the fatal landslide was determined based on the description of the landslide cause. For example, according to the description by the China Geological Hazard Bulletin, fatal landslide 1439 occurred at approximately 10:00 on July 24, 2010 in Qiaoergou, Gaobadian of Shanyang County, Shaanxi Province, which resulted in landslides due to heavy rainfall. This is an area prone to landsliding. The town of Gaobadian is located in the Qinba mountainous area, with steep mountains and slopes. The slope of the landslide is approximately 45–50 degrees with vegetation and an approximately 2–3 m thick, weathered soil layer. The underlying rock is metamorphic, such as

Table 1 Example of the FLEIC

ID	Date	Location	Latitude	Longitude	Radius of confidence (km)	Landslide type	Fatality	Trigger	Source
85	1958-12-16	Tonglu County, Hangzhou, Zhejiang Province	29.80	119.68	< 25	Generic shallow landslide	9	Unknown	Geological hazard event data set of China (1949-2008)
467	1990-06-14	Jinyuan, Dongchuan County, Kunming, Yunnan Province	103.14	25.85	< 10	Generic shallow landslide	20	Unknown	Geological hazard event data set of China (1949-2008)
1037	2005-07-21	Xiaocaoba, Yiliang County, Zhaotong, Yunnan Province	27.77	104.26	< 10	Rock fall	16	Rainfall and human activities	chinanews.com
1328	2009-05-17	Pingtang County, Qiannan Zhou, Guizhou Province	25.83	107.31	< 30	Generic shallow landslide	5	Rainfall	Yesterday Disaster Report
1439	2010-07-24	Qiaogou, Gaoba, Shanyang County, Shangluo City, Shaanxi Province	33.61	110.02	< 2	Generic shallow landslide	24	Rainfall	China Geological Hazard Bulletin
1813	2014-07-04	Mibei, Xinhuang County, Huaihua, Hunan Province	27.20	109.38	< 5	Generic shallow landslide	1	Rainfall	Reports on Geological Disaster Situation

calcareous slate. According to the meteorological report, the rainfall continued since July 16, including cumulative rainfall of 66.9 mm from 8 o'clock on July 23 to 5 o'clock on July 24. Based on the above, we attribute the trigger of fatal landslide event 1439 to the heavy rainfall. The fatalities caused by earthquake-triggered landslides are often attributed to the earthquakes. The actual fatalities caused by earthquake-triggered landslides can be underestimated based on the collection of fatal landslide data through media reports, geological hazard bulletin and online databases. For example, the May 12th, 2008 Wenchuan earthquake-triggered landslides in China were estimated to result in a quarter to one-third of all fatalities (Yin et al. 2009). These deaths were recorded as a result of the earthquake in media reports, geological hazard bulletin and other sources. We believe that the earthquake-triggered landslides in China need to be documented for each earthquake event through other data sources. Therefore, the fatal landslide inventory in this paper only contains the non-seismically triggered landslides.

Eventually, the Fatal Landslide Event Inventory of China (FLEIC) included a total of 1911 fatal landslide events for the period from 1950 to 2016, which resulted in a total of 28,139 fatalities. In the FLEIC, the majority of the fatal landslides are generic shallow landslides (1295, 67.8%), which are followed by debris flows (318, 16.6%) and rock falls (298, 15.6%). For the 1223 fatal landslides (64%) in the FLEIC, the trigger was rainfall, and for 78 (4.08%), the trigger was anthropogenic activity. In addition, 59 (3.09%) fatal landslide events were caused by rainfall and human activities, and 19 (0.99%) landslides were caused by other natural environment factors, such as snowmelt or a glacial lake outburst. The exact triggers for the remaining 532 events (27.8%) are still unknown, due to the lack of detailed descriptions of the causes. Compared to the fatal landslides in China recorded during the same period as the Emergency Events Database (EM-DAT), the fatal landslides in FLEIC were 26 times that of the EM-DAT (73 events) and the deaths in FLEIC were 5.1 times those contained in the EM-DAT (5568 deaths). This indicates that FLEIC can more fully reflect the losses caused by landslides in China. Compared with the statistics of landslides in the China Statistical Yearbook from 2000 to 2015, the number of fatalities in FLEIC for the same period was 8751, which accounts for 80% of the total number of deaths in the China Statistical Yearbook. For only the period from 2005 to 2015, the proportion rose to 97.4%. This shows that the FLEIC can present the impact of fatal landslide events in China.

Trend analysis

Sen's slope method

Sen's slope is a nonparametric method proposed by Sen (1968) to analyze trends in time series. The Sen's slope method is widely used in trend analyses of time series (Wu et al. 2016; Zhang et al. 2017). The advantage of this method is that the time series samples are not required to follow a specific distribution and are not susceptible to outliers. The formula is as follows:

$$\beta = \text{Median}\left(\frac{X_j - X_i}{j - i}\right), \quad \forall j > i \quad (1)$$

where β is the Sen's slope of the time series, x_j and x_i are elements in time j and i ($j > i$) of the time series to be analyzed, respectively,

and Median is the median function. When the result of β is greater than 0, the time series shows an increasing trend. When the result of β is less than 0, this indicates that the time series shows a decreasing trend.

Mann-Kendall test

The Mann-Kendall (MK) method is a nonparametric test method with the advantage that it is not susceptible to outliers (Kendall 1948; Mann 1945). The MK test method has been widely applied to test the significance of the trends in time series (Donat et al. 2013). The equation is as follows:

$$\begin{cases} S = \sum_{i=1}^{n-1} \sum_{j=i+1}^N \text{sign}(X_j - X_i) \\ \text{sign}(X_j - X_i) = \begin{cases} 1 & X_j - X_i > 0 \\ 0 & X_j - X_i = 0 \\ -1 & X_j - X_i < 0 \end{cases} \end{cases} \quad (2)$$

where S is the MK test statistic, x_j and x_i are the i and j values of the time series, respectively; and N is the length of the time series. If a data value from a later time period is higher than a data value from an earlier time period, the statistic S is incremented by 1. On the other hand, if the data value from a later time period is lower than a data value sampled earlier, S is decremented by 1. The net result of all such increments and decrements yields the final value of S (Shahid 2011). Then, the standard test statistic Z can be computed from Formula (2) to evaluate the presence of a statistically significant trend.

$$Z = \begin{cases} (S-1)/\sqrt{n(n-1)(2n+5)/18} & S > 0 \\ 0 & S = 0 \\ (S+1)/\sqrt{n(n-1)(2n+5)/18} & S < 0 \end{cases} \quad (3)$$

where the Z value is greater than 0, this indicates that the time series is on the rise; if the Z value is less than 0, this suggests that the time series is decreasing; and if the absolute value of the statistic Z is greater than 1.96, this indicates that the trend in a time series meets the 0.05 significance level.

Geographical detector method

The geographical detector method is a statistical method for spatial variance analysis (Wang et al. 2010; Luo et al. 2016). The core concept assumes that if an independent variable has a significant effect on a dependent variable, the spatial distribution of the independent and dependent variables should be similar (Wang and Xu 2017). The geographical detector method was first applied to health risk assessment (Wang et al. 2010), and then, the method was applied to the dissection density analysis (Luo et al. 2016), landslide susceptibility assessment (Luo and Liu 2017), and urbanization driving force analysis (Liu and Yang 2012). One of the advantages of the geographical detector method is that both continuous and categorical data can be analyzed. The formula is as follows:

$$q_x = 1 - \frac{1}{N\sigma^2} \sum_{h=1}^L N_h \sigma_h^2 \quad (4)$$

where the q_x value is the power of the determinant (PD) value for factor X , $h = 1, \dots, L$ is the category of the dependent variable Y or factor X ; N_h and N are the number of samples in category h and the total samples, respectively; and σ_h^2 and σ^2 are the variance of the dependent variable Y of category h and the variance of the entire area, respectively.

The range of q_x is 0 to 1. The larger the value of q_x , the closer the relationship between the independent variable X and the dependent variable Y . The q_x value is 1, which indicates that factor X completely controls the spatial distribution of Y . The q_x value is 0, which indicates that factor X has no relation to Y . The q_x value indicates the spatial variation proportion of Y explained by factor X . This method is used to detect the spatial association of X and Y rather than the direct causal relationship (Luo et al. 2016).

Another advantage of the geographical detector method is the ability to detect the interaction of two factors with the dependent variable. By calculating and comparing the q_x of a single factor and the q_x value after the two factors interact, it can be evaluated whether the interaction of the two factors will increase or decrease the explanatory power of dependent variable Y . More details can be found in these studies (Wang et al. 2010; Luo et al. 2016). In this paper, the geographical detector method was applied to detect the spatial association of the fatal landslide distribution in China and the natural environmental and human activity factors.

The dependent variable in this paper is the fatal landslide density of China, which can be calculated with the point density analysis function in the ArcGIS spatial analysis toolbox. The fatal landslide with a radius of confidence less than 25 km was used to calculate the density map. Then, the spatial distribution of the fatal landslide density of China is calculated using 25 km as the output raster cell and 3×3 pixels as the neighbor (Fig. 8).

The landslide spatial distribution is affected by many factors, which can be divided into seven categories (Lin et al. 2017a), including topography, geology, hydrology, soil, precipitation, land cover, and ground motion. In this study, we have selected 13 potential influencing factors (Fig. 8b–n), which can be roughly

divided into five categories: geology and soil property (lithology, faults, soil type, and soil erosion type), climate (precipitation), topography (elevation, slope, aspect, and curvature), land cover (normalized difference vegetation index (NDVI) and vegetation type), and human activity (road density, population density). The data sources and detailed information for each influencing factor are shown in Table 2.

For the geology factor, a new high resolution global lithological map was used to represent the rock properties and contains 15 lithological classes including unconsolidated sediment, siliciclastic sedimentary rock, pyroclastics, mixed sedimentary rock, carbonate sedimentary rock, evaporites, acid volcanics, intermediate volcanics, basic volcanics, acid plutonics, intermediate plutonics, basic plutonics, metamorphics, water bodies, ice, and glaciers (Hartmann and Moosdorf 2012). The distance from Quaternary active faults was calculated to represent the effect of geologic structures.

The soil type map has 12 soil classes, which include alfisols, semi-alfisols, pedocals, aridisols, desert soils, amorphous soils, semi-aqueous soil, aqueous soils, alkali-saline soils, anthrosols, Alpine soils, and ferrallisols. The soil erosion map is classified into three main classes: soil erosion by water, wind, and freeze-thaw, according to the type and nature of the dominant external erosion forces such as water, wind, freezing, and thawing. The reason we included the soil erosion factor is that soil erosion is the process of separation and transfer of soil particles under dominant natural erosion forces, which gradually develops in gully regions. With the slight loss of surface water and soil, rainfall infiltration in the slope area gradually formed a shallow landslide. Due to the constant infiltration of rainfall, the softening soil gradually formed a soft slip surface, and the landslide eventually became unstable. Some studies have investigated the application of the soil erosion model for a shallow landslide early warning system (Liang et al. 2015; Lu et al. 2017). Pradhan et al. (2012) also concluded that the soil erosion map can be used for shallow landslide hazard mapping. For the climate factor, the average annual precipitation for the period

Table 2 Potential factors influencing the spatial distribution of fatal landslides

Category	Factor	Description	Source
Climate	Precipitation	Average Annual Precipitation (1980~2010), 1 km resolution	http://www.resdc.cn
Geology and soil	Soil type	1 km resolution	http://www.resdc.cn
	Soil erosion type	1 km resolution	http://www.resdc.cn
	Lithology	1 km resolution	Hartmann and Moosdorf (2012)
	Distance from faults	1 km resolution	
Topography	Elevation	SRTM 90 m DEM resolution	http://srtm.csi.cgiar.org
	Slope	90 m resolution	Derived from DEM
	Curvature	90 m resolution	Derived from DEM
	Aspect	90 m resolution	Derived from DEM
Land cover	NDVI	Average Annual NDVI (1998~2015), 1 km resolution	http://www.resdc.cn
	Vegetation type	1 km resolution	http://www.resdc.cn
Human activity	Population density	Population distribution (2000), 1 km resolution	http://www.resdc.cn
	Road density	Road length in each county divided by the area and resampled to 1 km resolution	http://www.resdc.cn

from 1980 to 2010 was calculated to represent the landslide triggering condition.

The topography factors including elevation, slope, aspect, and curvature were calculated and used to represent the intrinsic landslide susceptibility condition. A digital elevation model (DEM) was obtained from the USGS/NASA Shuttle Radar Topographic Mission (SRTM) data. The SRTM payload was equipped on the Space Shuttle Endeavor. The SRTM uses interferometric synthetic aperture radar (InSAR) which measures Earth's elevation with two antennas. Using two radar antennas and a single pass, it generated a digital elevation model using InSAR. The SRTM data are available as 3 arcsec (approx. 90 m) DEM covering the globe from 60N to 60S. The 1 arcsec data product was also produced and are now available for all countries. To reduce the computer processing effort, the 90 m resolution DEM was used to derive the terrain parameters.

For the land cover factor, vegetation type and NDVI were adopted to represent the vegetation coverage property. The vegetation types include 11 classes such as taiga, mixed broadleaf-conifer forest, broad-leafed forest, brushwood, desert, grasslands, tussocks, meadow, swamp, Alpine vegetation, and cultivated vegetation. For the human activity factors, population density was adopted to represent the potential exposure population condition, and the road density was used to reflect the effects of human engineering activities on landslides.

Vegetation type, soil type, soil erosion type, aspect, and lithology are categorical variables which are directly used in the geographical detector

analysis. For continuous variables including precipitation, NDVI, elevation, slope, curvature, population density, and road density, the optimal discretization method was adopted to discretize continuous variables into categorical variables (Feng Cao et al. 2013). Specifically, five unsupervised discretization methods, including equal interval (EI), natural breaks (NB), quantile (QU), geometrical interval (GI), and standard deviation (SD), are used to divide all continuous variables into a number of classes. The number of discretization classes was set as 2–8 for each method. Then, the PD values for each of the discretization experiments were calculated and used to select the optimal classes for discretizing all continuous variables.

Finally, the zonal statistic function in the ArcGIS spatial analysis toolbox was used to obtain the zonal mean and zonal majority of the dependent variable and the independent variables, respectively. The output data from the zonal statistic can be used to detect the spatial association of the fatal landslide density and each factor in the geographical detector method.

Results

Temporal trends of fatal landslides

Figure 1a shows that during the period from 1950 to 2016, the frequency of fatal landslides that occurred in China was significantly increased, with a growth rate of 0.8 times/a ($P < 0.01$). The number of deaths caused by fatal landslides also showed a significant increasing trend, with a growth rate of 3 persons/a ($P < 0.05$). The frequency of fatal landslides in the past 20 years was significantly

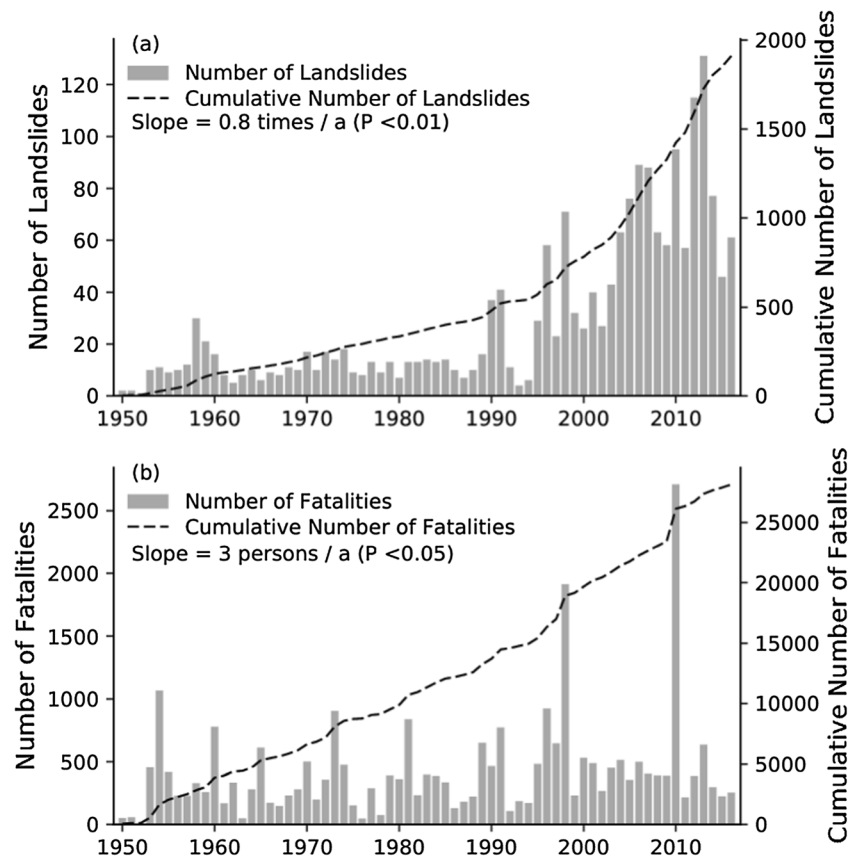


Fig. 1 Temporal variations in the frequency of fatal landslides and the resulting fatalities during 1950–2016

higher than that in the previous 40 years. Figure 1b shows that the fatalities caused by fatal landslides have fluctuated over the past 60 years. In the past 20 years, the fatalities caused by each fatal landslide have decreased. The frequency of fatal landslides and the number of deaths caused by fatal landslides during different periods were compared. The average annual frequencies of fatal landslides were 11, 31, and 68 for the periods 1950–1989, 1990–1999, and 2000–2016, respectively, and the average annual fatalities resulting from fatal landslides were 331, 589, and 530 for the three periods, respectively. The average fatalities caused by each fatal landslide were approximately 30 people during the period of 1950–1989, 19 people during the period of 1990–1999, and 8 people during the period of 2000–2016.

The long-term historical landslide database may have inherent incompleteness due to non-instrument records, which leads to a bias in the analysis. Specifically, for the fatal landslides that have caused a large number of fatalities and serious impacts, more attention would be paid to both the past and the current periods. However, fatal landslides with few fatalities may be neglected because information from the past was unavailable. To identify the impact of time series incompleteness and avoid this effect, the fatal landslides were divided into four grades for further analysis based on the number of deaths caused by each fatal landslide: very large (fatalities ≥ 30), large (10–30), medium (3–10), and small (< 3).

The fatal landslide proportion frequency in the four categories for the periods of 1950–1999 and 2000–2016 were different (Fig. 2a,

b). During the period of 1950–1999, the proportion of fatal landslides in the four categories were roughly equal. The proportion of medium fatal landslides is 33.9%. The proportion of very large, large, and small fatal landslides ranges from 20.5 to 23.8%. For the period from 2000 to 2016, the proportion of very large and large fatal landslides decreased to 3 and 11.9%, respectively. The proportion of medium and small fatal landslides increases to 38.1 and 46.9%.

From Fig. 2c, the interdecadal changes in the different classes of fatal landslide events show completely different trends. The very large fatal landslide events (fatalities ≥ 30) generally fluctuate between 1950 and 2016, rise from 1950 to 1999, and peak between 1990 and 1999, based on an average of 2.5 to 4.5 events per year. After the year 2000, there was a declining trend, with an average of 2.1 events per year. For the small and medium-sized fatal landslide events (fatalities < 10), a significant increasing trend is seen since 1950. Between 1950 and 1989, there were an average of 5.9 events per year, which rose to 18.8 events per year between 1990 and 1999. After 2000, the upward trend was even more pronounced. On average, approximately 57.8 fatal landslide events occurred every year.

This shows that a long time series landslide inventory has inconsistent records of fatal landslide events for different periods. From this, we can infer that the significant increasing trend of small and medium-sized fatal landslide events is partly due to the incompleteness of small

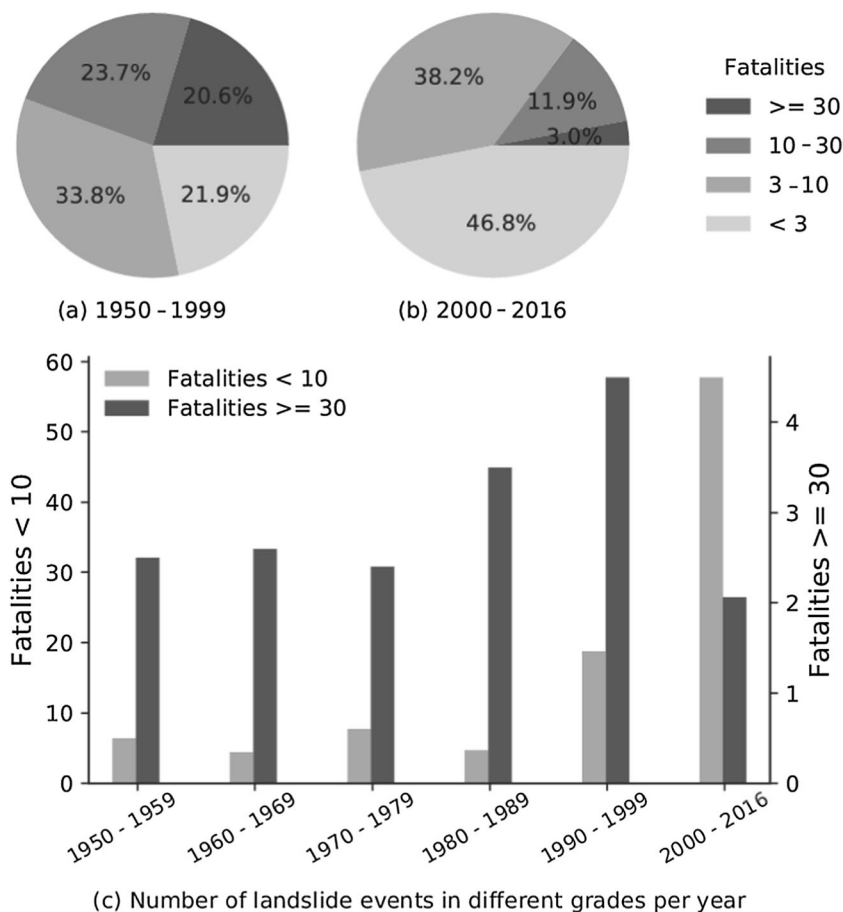


Fig. 2 The fatal landslide events in different grades for different periods

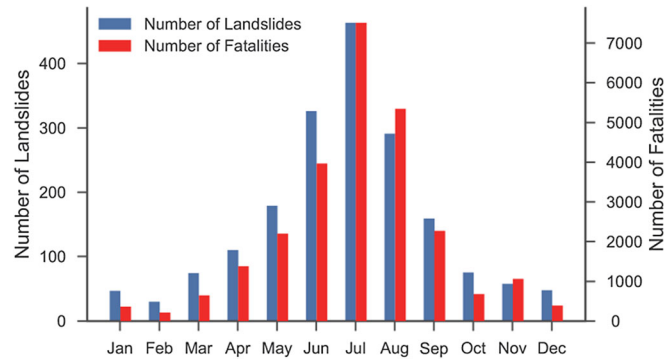


Fig. 3 Monthly variations in the frequency of fatal landslides and the resulting fatalities

and medium-scale fatal landslide events during the older-stage (mainly before 2000), which resulted in a proportion of very large and large fatal landslide events that was rather high during that period (Fig. 2a, b). The observed decrease in very large fatal landslide events (Fig. 2c) may be a result of the improvement of landslide disaster mitigation, prevention, and control. The statistics of the China Statistical Yearbook shows that the investment in geological disaster prevention and control increased annually, from 3.3×10^8 RMB in 2000 to 176×10^8 RMB in 2015 (Sheng et al. 2016). The geological disaster prevention and control projects also increased from 429 in 2000 to 26,289 in 2015.

The monthly variation in fatal landslide events is consistent with the monthly distribution of precipitation. The fatal landslides were mainly concentrated between April and September during 1950–2016, with a total frequency of 1528 (82.15%) fatal landslides, resulting in 22,655 (87.1%) deaths (Fig. 3). During the summer (June to August), there were

1080 (58.06%) fatal landslides, which resulted in 16,817 (64.65%) deaths. This was followed by the spring and autumn, with 363 (19.52%) and 292 (15.7%) fatal landslides, respectively, resulting in 4217 (16.21%) and 4010 (15.42%) fatalities, respectively. The frequency of fatal landslides in winter was the least, with a total of 125 (6.72%) times, which resulted in 967 (3.72%) deaths.

Spatial distribution of fatal landslides

Provincial scale

The fatal landslides were mainly distributed along the eastern margin of the Qinghai-Tibet Plateau along the junctions of the first and second slope-descending zone, the Loess Plateau, the middle reaches of the Yangtze River, the Sichuan Basin and its surrounding mountains, the Yunnan-Guizhou Plateau, and the southeast hilly area (Fig. 4). A number

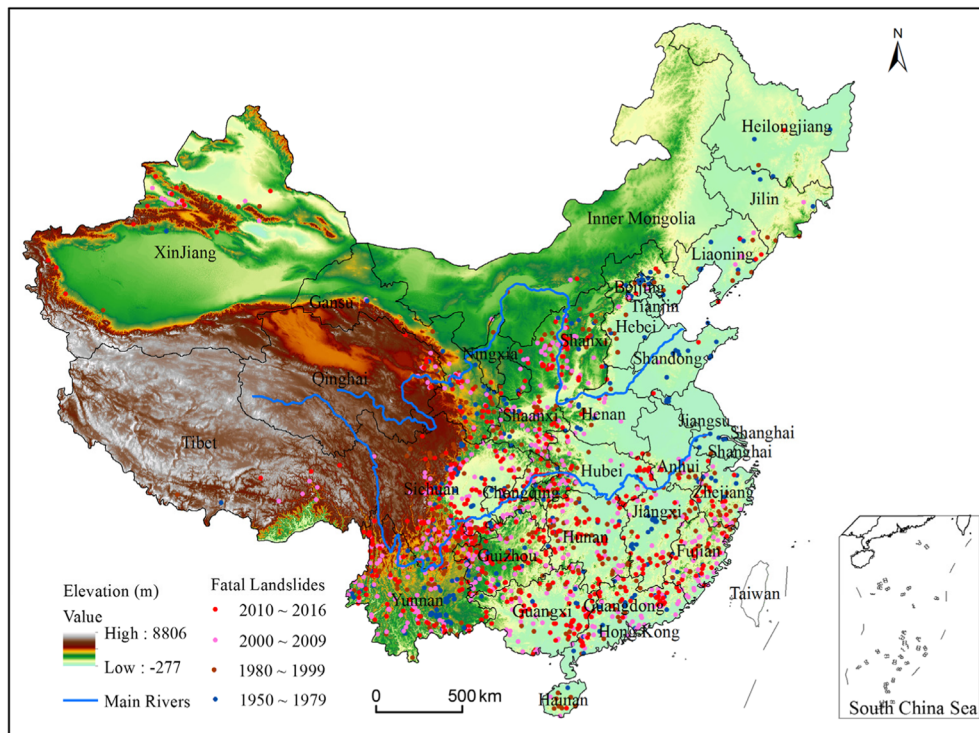


Fig. 4 Spatial distribution of fatal landslides in China

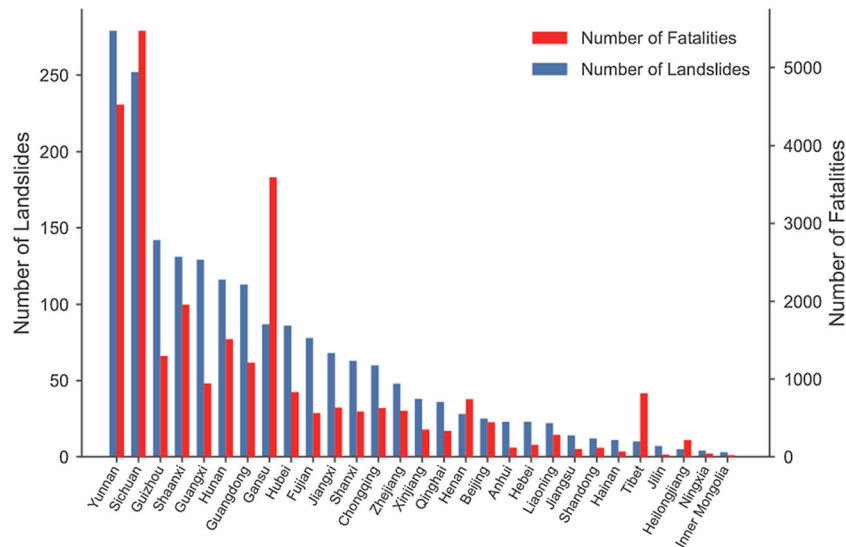


Fig. 5 The frequency of fatal landslides and the resulting fatalities in each province

of the fatal landslides occurred in the northwest Tianshan area, the western part of the Kunlun Mountains and the Northeast Changbai Mountain area.

The hotspot province of fatal landslides was in 14 provinces, which account for 86% of the total fatal landslides and resulting fatalities. These 14 provinces contain five southwestern provinces (Yunnan, Sichuan, Guangxi, Guizhou and Chongqing), five southeastern provinces (Hunan, Guangdong, Fujian, Jiangxi and Zhejiang), Shaanxi and Shanxi, Hubei and Gansu (Fig. 5). Specifically, fatal landslides most frequently occurred in the Yunnan and Sichuan Provinces with 277 and 253 events, respectively, resulting in the highest number of deaths, with 67 and 82 deaths per year, respectively. This was followed by Guizhou (142), Shaanxi (130), Guangxi (128), Hunan (116) and Guangdong (113), where the frequency of fatal landslides was more than 100 during the period from 1950 to 2016, and resulted in an average of 14 to 29 deaths per year. There were 87 fatal landslides that occurred in the Gansu Province, with an average annual number of 54 deaths. The main reason is that the Zhouqu debris flow resulted in 1768 deaths in 2010; if this catastrophic event is removed, the average annual deaths caused by fatal landslides in Gansu is 21. The provinces with frequent occurrences of fatal landslides include Hubei (86), Fujian (78), Jiangxi (68), Shanxi (62) and Chongqing (60), with an average of 8 to 12 deaths per year. In addition, in Henan and Tibet, the average annual number of deaths is more than 10, although only 30 and 10 fatal landslides occurred in these two provinces.

Geological environment region scale

According to the geological structure, geomorphology and climatic conditions of different regions in China, the China Geological Survey divided the country into seven geological environment regions. The seven geological environment regions include the northeastern wetland ecology region (NE), the Huang-Huaihai-Yangtze River Delta plain region (Yangtze), the South China bedrock hills region (SC), the northwest Loess

Plateau region (Loess), the southwest karst mountain region (SW), the northwest arid desert region (NW) and the permafrost region of the Qinghai-Tibet Plateau (Tibet).

On the geological environment region scale, fatal landslides are most frequently distributed in the SW region. The frequency of fatal landslides (874 events) and the resulting fatalities in the SW region are about half of China, which is followed by the SC region, the Loess region and Tibet region, where the occurrence frequencies were 526, 228 and 165, respectively. Specifically, a total of 874 (45.7%) fatal landslide events occurred in the SW region, resulting in 16,047 (57.0%) deaths, with an average annual of 13 events resulting in 240 deaths. A total of 526 fatal landslides occurred in the SC region, resulting in 4994 deaths, with an average of 7.9 times per year, which resulted in 75 deaths. The frequency of fatal landslides in the Loess region and Tibet region were 228 and 165, respectively, which resulted in 2976 and 2916 fatalities. There were 118 (6.2%) fatal landslides in the three areas of the Yangtze region, the NW region and the NE region, resulting in 1206 (4.3%) deaths.

Figure 6 shows the seasonal distribution of fatal landslides in each geological environment region. The occurrence frequency of fatal landslides is the highest in the summer, with a total of 1123 events, resulting in 18,846 deaths. The average annual frequency of fatal landslides during the summer is 16.8 events, accounting for 58.8% of the average annual frequency. The proportion of fatal landslides in the summer is above 60% for the NE region, Tibet region, and SW region; it is 49–53% for the SC region, Yangtze region, Loess region and NW region (Table 3). This is followed by the spring, where the frequency of fatal landslide is a total of 365 times (19.1% of the total), resulting in 4291 deaths and an average of 5.4 events per year resulting in 64 deaths. In the spring, the frequency of fatal landslides in the NW region and SC region accounted for 41 and 26% of the entire region, respectively. The frequency of fatal landslides in autumn and winter are 294 (15.4%) and 129 (6.8%), which resulted in 4020 and 982 deaths, respectively (Table 3).

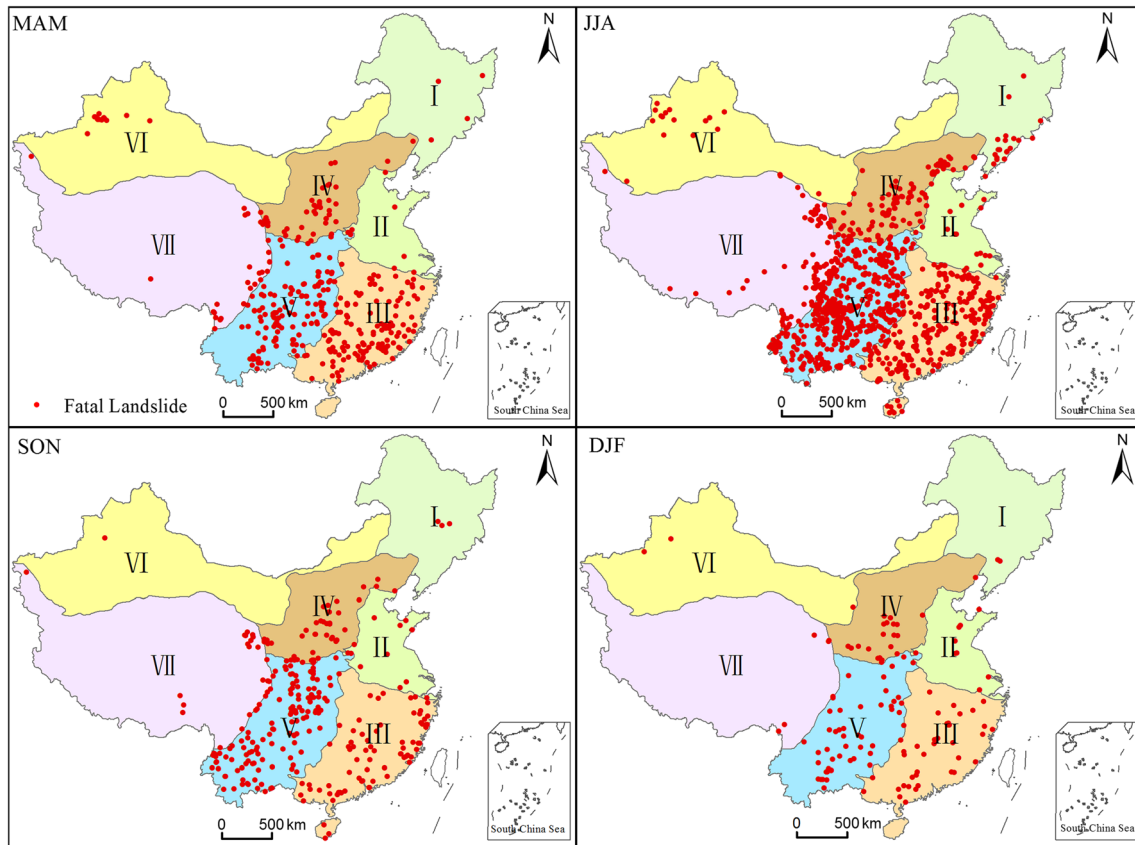


Fig. 6 Seasonal variations in fatal landslides in China (MAM: March, April, and May; JJA: June, July, and August; SON: September, October, and November; DJF: December, January, and February; I: the northeastern wetland ecology region (NE), II: the Huang-Huaihai-Yangtze River Delta plain region (Yangtze), III: the South China bedrock hills region (SC), IV: the northwest Loess Plateau region (Loess), V: the southwest karst mountain region (SW), VI: the northwest arid desert region (NW), and VII: the permafrost region of the Qinghai-Tibet Plateau (Tibet))

Possible influencing factors of fatal landslides

Before analyzing the roles of the potential influencing factors on fatal landslide events, the correlation coefficients between the six continuous variables were calculated. The results showed that the correlations were higher with rainfall and NDVI (0.67), elevations and NDVI (-0.47), and the absolute values of the correlation coefficients between other influencing factors were all less than 0.35. Moreover, the principle of the geographical detector method ensures that it is immune to the collinearity of multiple independent variables. Therefore, it is appropriate to include the above continuous variables and categorical variables in the analysis.

Figure 7 shows the distribution of fatal landslide events for all potential influencing factors. For precipitation, road density, population density, and NDVI factors, the distribution density of fatal landslide events increases with an increase in the average annual precipitation, road density, population density, and vegetation coverage. For distance from Quaternary active faults, the fatal landslide density tends to decrease with increasing distance from the faults. For the slope factor, the most frequent fatal landslide events are areas with a slope of 15–25 degrees, which is followed by 5–15 degrees. The density of fatal landslide events decreases with increasing elevation, but there are fatal landslide-prone zones in areas with altitudes of 150–500 m and 1500–3000 m. For terrain

curvature factors, fatal landslide events occur more frequently in the concave and convex areas. Regarding the aspect factor, there is no significant difference in the frequency of fatal landslide events for each aspect. For the soil type factors, the density of fatal landslides occurred more frequently in the six soil types including ferrallisols, semi-alfisols, anthrosols, alfisols, amorphic soil and pedocals. For the soil erosion factor, the density of fatal landslide events was much higher in areas with soil erosion by water forces compared to soil erosion by wind or freeze-thaw, and the greater the intensity of water forces, the more prone the area to fatal landslide events. For the vegetation type factors, the density of fatal landslides in tussocks, brushwood, taiga, cultivated vegetation and broad-leaved forests is higher than other vegetation types. For lithologic factors, the density of fatal landslides more frequently occurred in the five lithologies of carbonate sedimentary rock, mixed sedimentary rock, metamorphics, pyroclastics, siliciclastic sedimentary rock, and acid plutonics.

Table 4 shows the q statistic of the possible influencing factors and their interactions with the spatial distribution of fatal landslides, which is based on the geographical detector method. For the precipitation factor, we only analyzed the interactions effect with other influencing factors on fatal landslide events due to the precipitation factor's role of trigger. For the role of single

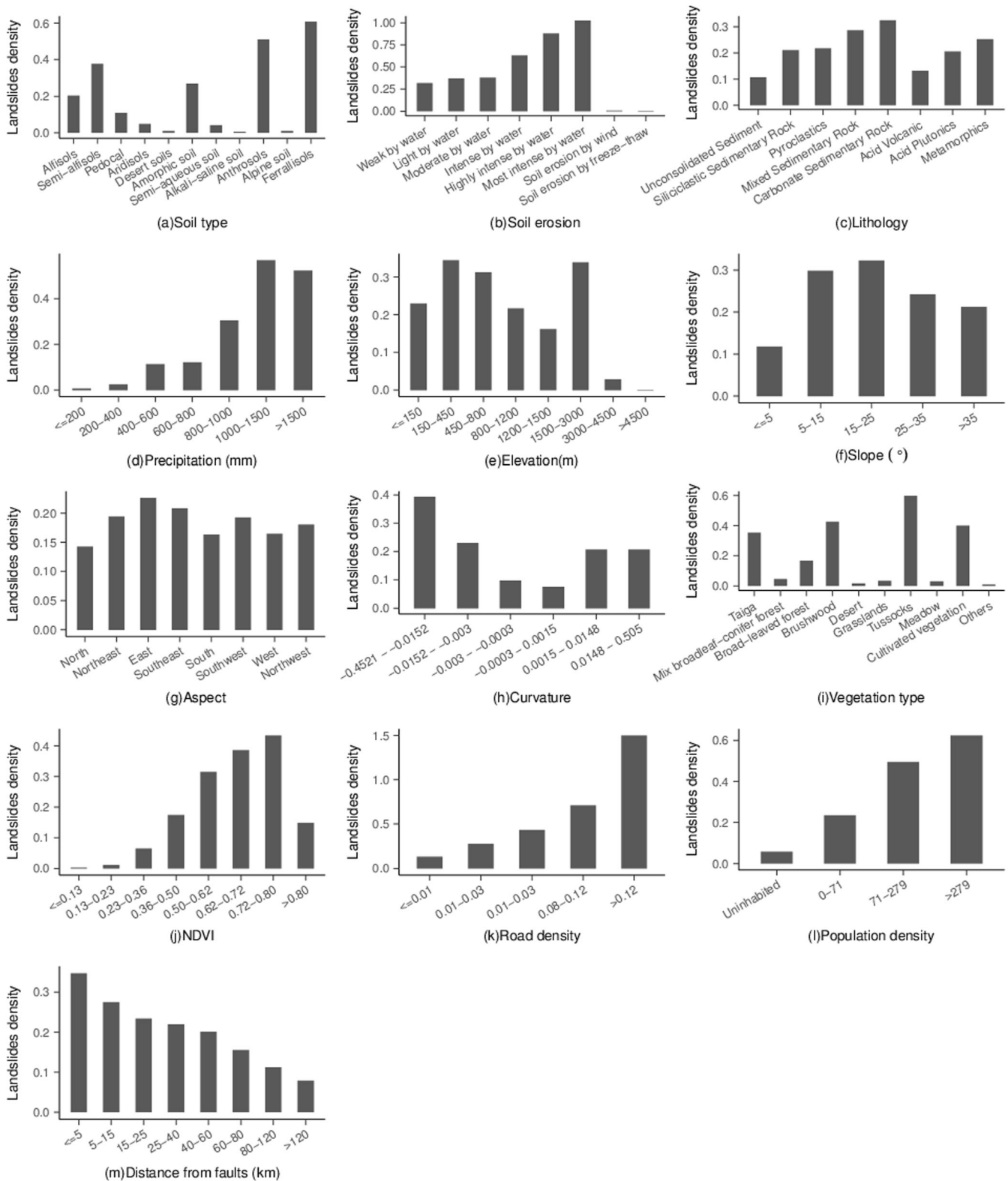


Fig. 7 The relationship between potential influencing factors and fatal landslide events

frequency of fatal landslide events at different grades revealed significant differences. The very large fatal landslide events (fatalities ≥ 30) generally fluctuated between 1950 and 2016, showing

an increasing trend from 1950 to 1999. After 2000, there is a decreasing trend. However, the small and medium-sized fatal landslide events (fatalities < 10) showed a significant increasing

Table 4 The *q* statistic of possible influencing factors and their interactions

Factors	<i>q</i> statistic	Factor interaction	<i>q</i> statistic
Vegetation type	0.27	Precipitation ∩ elevation	0.49
Soil type	0.26	Precipitation ∩ soil type	0.46
Soil erosion	0.21	Precipitation ∩ slope	0.43
NDVI	0.21	Precipitation ∩ lithology	0.41
Slope	0.18	Precipitation ∩ vegetation type	0.41
Curvature	0.17	Precipitation ∩ population density	0.40
Population density	0.14	Soil type ∩ slope	0.46
Elevation	0.12	Soil type ∩ curvature	0.42
Road density	0.10	Vegetation type ∩ soil type	0.42
Aspect	0.08	Vegetation type ∩ elevation	0.42
Lithology	0.05		
Faults	0.03		

trend between 1950 and 2016. After 2000, the increasing trend was even more pronounced. One of the reasons for the different trends

in fatal landslide events at different grades is because of the inconsistent records of landslide events at different grades in the

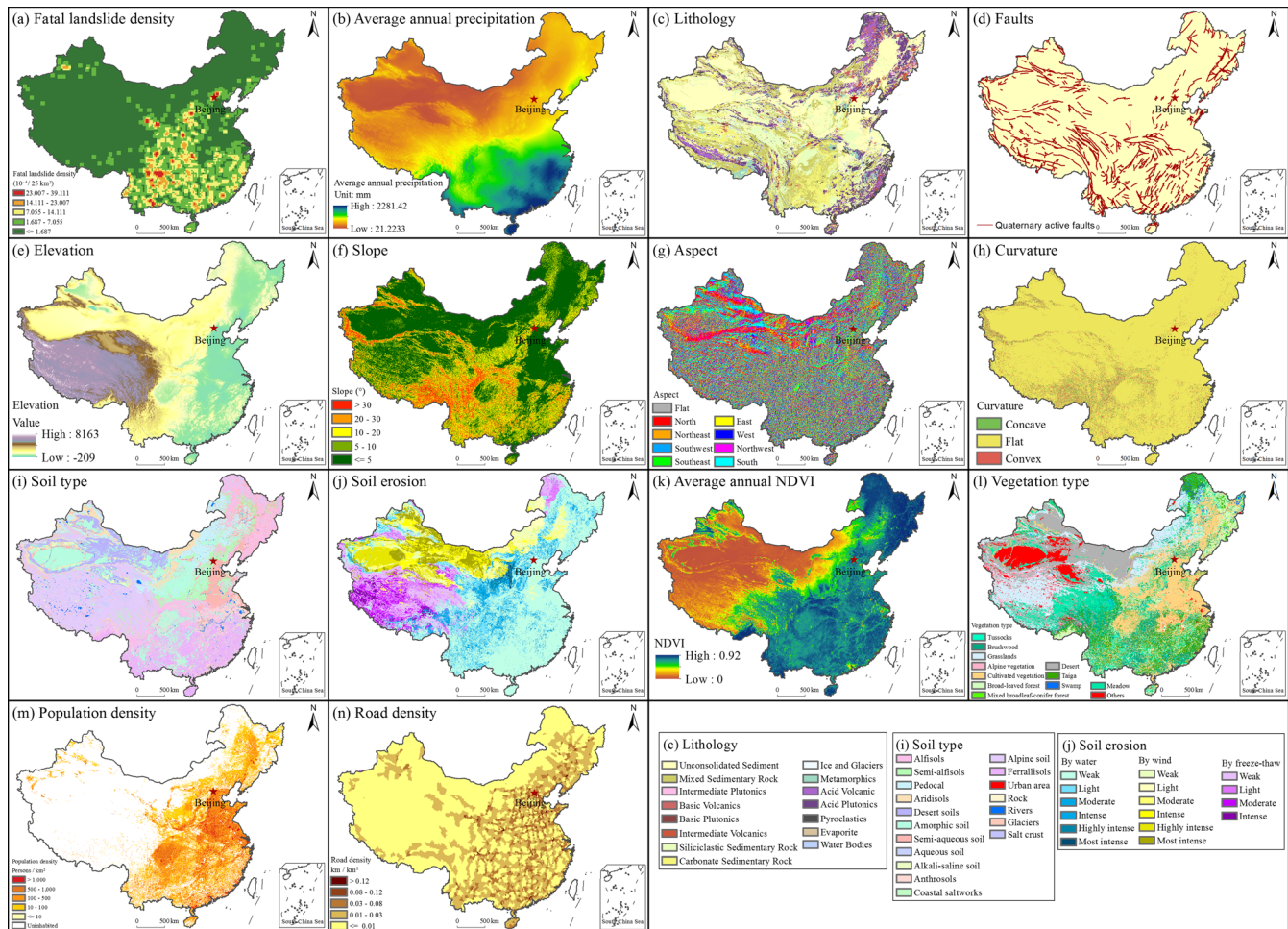


Fig. 8 Distribution map of a fatal landslide density; b average annual precipitation (1981~2010); c lithology; d faults; e elevation; f slope; g aspect; h curvature; i soil type; j soil erosion; k average annual NDVI (1998~2015); l vegetation type; m population density; and n road density

long-term landslide inventory. For very large fatal landslide events, the long-term record is generally complete. The decreasing trend after 2000 can be attributed to the investment increase in landslide mitigation measures. This is also proven by the annual increases from 2000 to 2015 in geological disaster prevention investment and geological disaster prevention and control projects in the statistical yearbook data from 2000 to 2015 (Sheng et al. 2016). This suggests that these geological disaster prevention and mitigation investments can reduce losses resulting from fatal landslides. The government should continue to strengthen disaster prevention and control efforts.

For the small and medium-sized fatal landslide events, the occurrence frequency has increased significantly, which is especially apparent in the increasing trend since 2000 as there has been an improvement in the availability of landslide data online. This may also be related to a number of other factors, including an increase in extreme precipitation events in China over the past 50 years (Wang and Zhou 2005; Zhai et al. 2005); an increase in surface loose material and in exposed population, which results from the effects of land urbanization (Li et al. 2017); and an increase in landslides caused by climate change (Gariano and Guzzetti 2016). We have not been able to quantify the contribution of these factors to the rising trend of small and medium-sized fatal landslide events. There is also a need for more complete and adequate regional landslide data to explore the causes of fatal landslide trends. The above analysis also suggests that we should pay special attention to the possible impact of database incompleteness when analyzing long-term trends.

The monthly distribution of fatal landslide events shows that 82.15% of the fatal landslides are concentrated between April and September. The distribution characteristics are closely related to the monthly variation in precipitation in China. For example, 95.6% of the extreme precipitation events in China are concentrated between April and September (Fu et al. 2013). Therefore, the FLEIC can also be used to combine the meteorological observation precipitation or satellite precipitation data to further explore the relationship between extreme precipitation and fatal landslides.

The results of the spatial pattern analysis of the fatal landslide in China show that the fatal landslides are mainly distributed in five provinces in southwestern China (Yunnan, Sichuan, Guangxi, Guizhou and Chongqing), five provinces in southeastern China (Hunan, Guangdong, Fujian, Jiangxi and Zhejiang), Shaanxi and Shanxi, Hubei and Gansu. These 14 provinces are responsible for 86% of the total fatal landslides and the resulting fatalities during 1950–2016. On the geological environment region scale, the fatal landslides most frequently occurred in the southwest karst mountain region. The occurrence frequency proportion of fatal landslides was 45.7%. This was followed by the South China bedrock hills region, the northwest Loess Plateau region and the permafrost region of the Qinghai-Tibet Plateau, with the proportions of 27.5%, 11.9 and 8.6% respectively. These provinces and regions should further increase their investments in landslide disaster prevention and mitigation and landslide risk research, to better reduce the frequency of fatal landslides and the resulting losses.

The spatial relationship between the fatal landslide density, natural environment and human activity factors are analyzed using the new method of the geographical detector. The q value of the factor interaction between precipitation and topography, soil type, lithology, vegetation type, population density and other

factors is greater than the q statistic values of all individual factors, which indicates that the causes of fatal landslide events in China are complex and diverse and are more closely related to the interactions of many factors. In the process of landslide susceptibility, hazard and risk assessment, more consideration should be given to the effects of multi-factor interactions.

With regard to the Modifiable Areal Unit Problem (MAUP) that may be caused by different spatial scales (Openshaw 1984; Swift et al. 2008), the spatial pattern analysis shows that the distribution of the fatal landslide events on the provincial and the geological environment region scales are nearly consistent. Over 70% of the fatal landslide events and resulting deaths are concentrated in southwest and southeast China. Based on the Sen's slope method, the frequencies of fatal landslide events in different geological environment regions were analyzed. The results show that the trend of fatal landslide events has been consistent with the national trend, which shows an increasing trend in five regions including SW, SC, Loess, NE and Tibet region. We have also attempted to apply the geographical detector method to explore the relationship between potential influencing factors and the distribution of fatal landslide events in different geological environment regions. However, since too few data are allocated to each region, we cannot separately analyze each zone. This requires further gathering of a richer regional database to explore this issue.

The research of some scholars also shows that there were many landslides that would not have occurred without an earthquake, even though they moved many months later (Lin et al. 2006; Zhang et al. 2014). Therefore, taking the 2008 Wenchuan earthquake disaster area as an example, we used the 184 fatal landslide events that occurred in the earthquake intensities and damage area between 1950 and 2016 to explore the possible impact of large earthquakes on non-earthquake-induced fatal landslide events. After the 2008 Wenchuan earthquake, the average annual frequency of fatal landslide events increased from 1.86 events (1950–2007) to 8.44 events (2008–2016). Looking at the situation just 10 years before the Wenchuan earthquake, the average annual frequency of fatal landslides also increased from 4.1 (1998–2007) to 8.44 (2008–2016). Specifically, the small and medium-sized fatal landslide events increased from an average of 0.93 to 7.11 times per year, and the very large and large fatal landslide events rose from an average of 0.93 to 1.33 per year. However, from the previous analysis, we know that since the year 2000 very large landslides in China have shown a decreasing trend. The precipitation changes before and after the 2008 Wenchuan earthquake were also calculated. The results showed that there was no significant increase in the average annual precipitation in the Wenchuan earthquake affected area (1950–2007: 965 mm and 2008–2016: 967 mm). This shows that large earthquakes will indirectly increase the frequency of fatal landslides in earthquake-stricken areas in coming years, especially increases in large fatal landslide events. Therefore, it is necessary to strengthen the risk prevention and management of landslide hazards in earthquake-stricken areas in Sichuan, Yunnan, and Gansu Provinces, where large earthquakes have occurred in recent years.

The FLEIC, which was established in this study, also has two aspects of future research that need to be further improved. One is that the economic losses caused by landslides should be collected and analyzed, as the spatial and temporal characteristics of economic losses may be different from the characteristics of fatalities.

We also attempt to collect and analyze the direct economic losses caused by fatal landslide events since 2000. The results show that from 2000 to 2016, the direct economic losses caused by fatal landslide events have ranged from 4 million to 1255 million RMB per year, and caused an average annual loss of about 313 million RMB. From the perspective of its spatial distribution, Sichuan and Yunnan provinces in the southwestern region suffered the most serious economic losses due to fatal landslides, with an average annual loss of about 78 million RMB. This is followed by Gansu, Shaanxi, Xinjiang, Hunan and Liaoning, the average annual economic loss is about 15–34 million RMB. The annual economic losses in the five provinces of Tibet, Guizhou, Chongqing, Hubei and Henan are 5.9–8.6 million RMB. These results reveal that there are still some differences in the spatial pattern between economic losses and casualties caused by fatal landslide events. However, considering the difficulty in obtaining economic loss data, these analyses of the economic loss caused by fatal landslide events may have a certain degree of underestimation, and more complete data needs to be collected for further analysis. Second, the FLEIC only includes non-earthquake induced fatal landslides, and further extension of the FLEIC should collect and analyze the significant earthquake-triggered landslide events in China.

Conclusions

In this paper, 1911 non-earthquake induced fatal landslides, which occurred during 1950–2016, were collected from multiple sources and developed into a nearly complete long-term fatal landslide database for the first time in China, known as FLEIC. Based on the spatiotemporal variation analysis of fatal landslides in FLEIC, the following conclusions are drawn.

- (1) Compared with the EM-DAT database and the statistics of the China Statistical Yearbook, the database is relatively complete and can be used to quantitatively analyze the spatial and temporal patterns of fatal landslide events in China and improve landslide hazard and risk assessment and as well as the analysis of its influencing factors.
- (2) There is a significant difference in the interdecadal trends in the frequency of fatal landslide events at different grades due to the inconsistent records of landslide events at different grades in the long-term landslide inventory. The very large fatal landslide events (fatalities ≥ 30) rose during 1950–1999 and declined in 2000–2016. The decreasing trend after the year 2000 can be attributed to the increase in landslide mitigation investments. The small and medium-sized fatal landslide events (fatalities < 10) showed a significant increasing trend between 1950 and 2016, especially during the period of 2000–2016. This significant increasing trend is partly due to the improvement of the availability of landslide data online. This inspires us to consider the possible effects of the inherent incompleteness of historical database when analyzing landslide historical records. The monthly distribution of fatal landslides in the FLEIC is consistent with the monthly variation in precipitation in China, mainly from April to September (82.15%).
- (3) A total of 86% of the fatal landslides and resulting loss of lives occurred in 14 provinces including five provinces in southwestern China (Yunnan, Sichuan, Guangxi, Guizhou and Chongqing), five provinces in southeastern China (Hunan,

Guangdong, Fujian, Jiangxi and Zhejiang), Shaanxi and Shanxi, Hubei and Gansu. According to the geological environment region, 45.7% of the fatal landslides events were distributed in the southwest karst mountain region, followed by the South China bedrock hills region, the northwest Loess Plateau region and the permafrost region of the Qinghai-Tibet Plateau, the proportions of which were 27.5%, 11.9 and 8.6%, respectively.

- (4) The role of individual influencing factors including geology and soil properties, climate, topography, land cover and human activities are related to the spatial distribution of fatal landslide events but their effects are limited. The factor interaction between precipitation and altitude, soil type, lithology type, vegetation type and population density have a greater impact on the spatial patterns of fatal landslides in China.

Acknowledgements

This work was supported primarily by the National Key Research and Development Program of China [No. 2016YFA0602403, No. 2017YFC1502505] and the National Natural Science Funds [41271544]. Acknowledgement for the data support from “National Earth System Science Data Sharing Infrastructure, National Science & Technology Infrastructure of China. (<http://www.geodata.cn>)” and Data Center for Resources and Environmental Sciences, Chinese Academy of Sciences (RESDC). Finally, we would like to thank the three anonymous reviewers and the handling editor for their valuable comments and suggestions, which helped to improved the manuscript.

References

- Cao F, Ge Y, Wang J-F (2013) Optimal discretization for geographical detectors-based risk assessment. *GISci Remote Sens* 50:78–92. <https://doi.org/10.1080/15481603.2013.778562>
- China Institute for Geo-Environment Monitoring (CIGEM) (2016) China geological hazard bulletin 2016. China Geological Environmental Monitoring Institute Web. <http://www.cigem.gov.cn/>. Accessed 10 Aug 2017. (in Chinese)
- Damm B, Klose M (2015) The landslide database for Germany: closing the gap at national level. *Geomorphology* 249:82–93. <https://doi.org/10.1016/j.geomorph.2015.03.021>
- Donat MG, Alexander LV, Yang H, Durre I, Vose R, Caesar J (2013) Global land-based datasets for monitoring climatic extremes. *Bull Am Meteorol Soc* 94:997–1006. <https://doi.org/10.1175/BAMS-D-12-00109.1>
- Fu G, Yu J, Yu X, Quyang R, Zhang Y, Wang P, Liu W, Min L (2013) Temporal variation of extreme rainfall events in China, 1961–2009. *J Hydrol* 487:48–59. <https://doi.org/10.1016/j.jhydrol.2013.02.021>
- Gariano SL, Guzzetti F (2016) Landslides in a changing climate. *Earth Sci Rev* 162:227–252. <https://doi.org/10.1016/j.earscirev.2016.08.011>
- Guzzetti F (2000) Landslide fatalities and the evaluation of landslide risk in Italy. *Eng Geol* 58:89–107. [https://doi.org/10.1016/S0013-7952\(00\)00047-8](https://doi.org/10.1016/S0013-7952(00)00047-8)
- Guzzetti F, Mondini AC, Cardinali M, Fiorucci F, Santangelo M, Chang KT (2012) Landslide inventory maps: new tools for an old problem. *Earth Sci Rev* 112:42–66. <https://doi.org/10.1016/j.earscirev.2012.02.001>
- Haque U, Blum P, da Silva PF, Andersen P, Pilz J, Chalov SR, Malet JP, Aulicié MJ, Andres N, Poyiadji E, Lamas PC, Zhang W, Peshevski I, Pétursson HG, Kurt T, Dobrev N, García-Davalillo JC, Halkia M, Ferri S, Gaprindashvili G, Engström J, Keellings D (2016) Fatal landslides in Europe. *Landslides* 13:1545–1554. <https://doi.org/10.1007/s10346-016-0689-3>
- Hartmann J, Moosdorf N (2012) The new global lithological map database GLiM: a representation of rock properties at the earth surface. *Geochem Geophys Geosyst* 13:1–37. <https://doi.org/10.1029/2012GC004370>

- Kendall MG (1948) Rank correlation methods. Griffin, Oxford
- Kirschbaum DB, Adler R, Hong Y, Hill S, Lerner-Lam A (2010) A global landslide catalog for hazard applications: method, results, and limitations. *Nat Hazards* 52:561–575. <https://doi.org/10.1007/s11069-009-9401-4>
- Kirschbaum D, Stanley T, Zhou Y (2015) Spatial and temporal analysis of a global landslide catalog. *Geomorphology* 249:4–15. <https://doi.org/10.1016/j.geomorph.2015.03.016>
- Klose M, Damm B, Highland LM (2015) Databases in geohazard science: an introduction. *Geomorphology* 249:1–3. <https://doi.org/10.1016/j.geomorph.2015.06.029>
- Klose M, Maurischat P, Damm B (2016) Landslide impacts in Germany: a historical and socioeconomic perspective. *Landslides* 13:183–199. <https://doi.org/10.1007/s10346-015-0643-9>
- Li WY, Liu C, Hong Y, Zhang XH, Wan ZM, Saharia M, Sun WW, Yao DJ, Chen W, Chen S, Yang XQ, Yue Y (2016) A public cloud-based China's landslide inventory database (CsLID): development, zone, and spatiotemporal analysis for significant historical events, 1949–2011. *J Mt Sci* 13:1275–1285. <https://doi.org/10.1007/s11629-015-3659-7>
- Li G, Lei Y, Yao H, Wu S, Ge J (2017) The influence of land urbanization on landslides: an empirical estimation based on Chinese provincial panel data. *Sci Total Environ* 595:681–690. <https://doi.org/10.1016/j.scitotenv.2017.03.258>
- Liang Y, Liu J, Li L et al (2015) Study of estimating critical rainfall of landslide based on soil erosion model. *Resour Environ Yangtze Basin* 24(03):464–468 (Chinese with English abstract)
- Lin CW, Liu SH, Lee SY, Liu CC (2006) Impacts of the Chi-Chi earthquake on subsequent rainfall-induced landslides in central Taiwan. *Eng Geol* 86(2–3):87–101
- Lin L, Lin Q, Wang Y (2017a) Landslide susceptibility mapping on a global scale using the method of logistic regression. *Nat Hazards Earth Syst Sci* 17:1411–1424. <https://doi.org/10.5194/nhess-17-1411-2017>
- Lin Q, Wang Y, Liu T, Zhu Y, Sui Q (2017b) The vulnerability of people to landslides: a case study on the relationship between the casualties and volume of landslides in China. *Int J Environ Res Public Health* 14:212. <https://doi.org/10.3390/ijerph14020212>
- Liu Y, Yang R (2012) Spatial characteristics and mechanisms of county level urbanization in China. *Acta Geograph Sin* 67:1011–1020 (Chinese with English abstract)
- Lu J, Fan W, Lu Y (2017) Research on early warning of shallow landslide based on soil erosion model. *Bull Soil Water Conserv* 37(3):227–230 (Chinese with English abstract)
- Luo W, Liu CC (2017) Innovative landslide susceptibility mapping supported by geomorphon and geographical detector methods. *Landslides* 15:1–10. <https://doi.org/10.1007/s10346-017-0893-9>
- Luo W, Jasiewicz J, Stepinski T, Wang J, Xu C, Cang X (2016) Spatial association between dissection density and environmental factors over the entire conterminous United States. *Geophys Res Lett* 43:692–700. <https://doi.org/10.1002/2015GL066941>
- Mann HB (1945) Nonparametric tests against trend. *Econometrica* 13:245–259. <https://doi.org/10.2307/1907187>
- Ministry of Land and Resources of China (MLRC) (2017) Report on geological disaster situation. Ministry of Land and Resources of China Web. http://www.mlr.gov.cn/dzhj/dzzh/zqxqbg/201706/t20170626_1512282.htm. Accessed 10 Aug 2017. (in Chinese)
- Nadim F, Kjekstad O, Peduzzi P, Herold C, Jaedicke C (2006) Global landslide and avalanche hotspots. *Landslides* 3:159–173. <https://doi.org/10.1007/s10346-006-0036-1>
- Openshaw S (1984) Concepts and techniques in modern geography. Geobooks, Norwich
- Pennington C, Freeborough K, Dashwood C, Dijkstra T, Lawrie K (2015) The National Landslide Database of Great Britain: acquisition, communication and the role of social media. *Geomorphology* 249:44–51. <https://doi.org/10.1016/j.geomorph.2015.03.013>
- Pereira S, Zêzere JL, Quaresma I, Santos PP, Santos M (2016) Mortality patterns of hydro-geomorphologic disasters. *Risk Anal* 36(6):1188–1210
- Petley DN (2010) On the impact of climate change and population growth on the occurrence of fatal landslides in South, East and SE Asia. *Q J Eng Geol Hydrogeol* 43:487–496. <https://doi.org/10.1144/1470-9236/09-001>
- Petley DN (2012) Global patterns of loss of life from landslides. *Geology* 40:927–930. <https://doi.org/10.1130/G33217.1>
- Pradhan B, Chaudhari A, Adinarayana J, Buchroithner MF (2012) Soil erosion assessment and its correlation with landslide events using remote sensing data and GIS: a case study at Penang Island, Malaysia. *Environ Monit Assess* 184(2):715–727. <https://doi.org/10.1007/s10661-011-1996-8>
- Sen PK (1968) Estimates of the regression coefficient based on Kendall's tau. *J Am Stat Assoc* 63:1379–1389. <https://doi.org/10.1080/01621459.1968.10480934>
- Sepúlveda SA, Petley DN (2015) Regional trends and controlling factors of fatal landslides in Latin America and the Caribbean. *Nat Hazards Earth Syst Sci* 15:1821–1833. <https://doi.org/10.5194/nhess-15-1821-2015>
- Shahid S (2011) Trends in extreme rainfall events of Bangladesh. *Theor Appl Climatol* 104(3–4):489–499. <https://doi.org/10.1007/s00704-010-0363-y>
- Sheng L, Wang W, Zhu W (2016) China statistical yearbook 2016. China Statistics Press, Beijing (in Chinese)
- Swift A, Liu L, Uber J (2008) Reducing MAUP bias of correlation statistics between water quality and GI illness. *Comput Environ Urban Syst* 32(2):134–148
- Taylor FE, Malamud BD, Freeborough K, Demeritt D (2015) Enriching Great Britain's national landslide database by searching newspaper archives. *Geomorphology* 249:52–68. <https://doi.org/10.1016/j.geomorph.2015.05.019>
- Van Den Eckhaut M, Hervás J (2012) State of the art of national landslide databases in Europe and their potential for assessing landslide susceptibility, hazard and risk. *Geomorphology* 139:545–558. <https://doi.org/10.1016/j.geomorph.2011.12.006>
- Wang J, Xu C (2017) Geodetector: principle and prospective. *Acta Geograph Sin* 72:116–134 (Chinese with English abstract)
- Wang Y, Zhou L (2005) Observed trends in extreme precipitation events in China during 1961–2001 and the associated changes in large-scale circulation. *Geophys Res Lett* 32:L09707. <https://doi.org/10.1029/2005GL022574>
- Wang JF, Li XH, Christakos G, Liao YL, Zhang T, X G, Zheng ZY (2010) Geographical detectors-based health risk assessment and its application in the neural tube defects study of the Heshun Region, China. *Int J Geogr Inf Sci* 24:107–127. <https://doi.org/10.1080/13658810802443457>
- Wu Y, Wu SY, Wen, Xu M, Tan J (2016) Changing characteristics of precipitation in China during 1960–2012. *Int J Climatol* 36:1387–1402. <https://doi.org/10.1002/joc.4432>
- Yin Y, Wang F, Sun P (2009) Landslide hazards triggered by the 2008 Wenchuan earthquake, Sichuan, China. *Landslides* 6:139–152. <https://doi.org/10.1007/s10346-009-0148-5>
- Zhai P, Zhang X, Wan H, Pan X (2005) Trends in total precipitation and frequency of daily precipitation extremes over China. *J Clim* 18:1096–1108. <https://doi.org/10.1175/JCLI-3318.1>
- Zhang S, Zhang LM, Glade T (2014) Characteristics of earthquake-and rain-induced landslides near the epicenter of Wenchuan earthquake. *Eng Geol* 175:58–73
- Zhang M, Du S, Wu Y, Wen J, Wang C, Xu M, Wu SY (2017) Spatiotemporal changes in frequency and intensity of high-temperature events in China during 1961–2014. *J Geogr Sci* 27:1027–1043. <https://doi.org/10.1007/s11442-017-1419-z>

Electronic supplementary material The online version of this article (<https://doi.org/10.1007/s10346-018-1037-6>) contains supplementary material, which is available to authorized users.

Q. Lin · Y. Wang (✉)

Key Laboratory of Environmental Change and Natural Disaster of Ministry of Education, Beijing Normal University,
No.19, Xijiekouwai Street, HaiDian District, Beijing, 100875, People's Republic of China
Email: wy@bnu.edu.cn

Q. Lin · Y. Wang

State Key Laboratory of Earth Surface Processes and Resource Ecology,
Beijing Normal University,
Beijing, 100875, China

Q. Lin · Y. Wang

Academy of Disaster Reduction and Emergency Management,
Beijing Normal University,
Beijing, 100875, China